Jelly-Z: Twisted and coiled polymer muscle actuated jellyfish robot for environmental monitoring

Pawandeep Singh Matharu[1], Akash Ashok Ghadge[1], Yara Almubarak[2], Yonas Tadesse[1,3,4,5]

[1] *Humanoids, Biorobotics, and Smart Systems Laboratory, Mechanical Engineering Department, The University of Texas at Dallas, Richardson, TX 78705, USA*

[2] *SoRobotics Laboratory, Mechanical Engineering Department, Wayne State University, Detroit, MI 48202, USA*

[3] *Biomedical Engineering Department, The University of Texas at Dallas, Richardson, TX 78705, USA*

[4] *Electrical and Computer Engineering Department, The University of Texas at Dallas, Richardson, TX 78705, USA*

[5] *Alan G. MacDiarmid Nanotech Institute, The University of Texas at Dallas, Richardson, TX 78705, USA*

ABSTRACT
Silent underwater actuation and object detection are desired for certain applications in environmental monitoring. However, several challenges need to be faced when addressing simultaneously the issues of actuation and object detection using vision system. This paper presents a swimming underwater soft robot inspired by the moon jellyfish (Aurelia aurita) species and other similar robots; however, this robot uniquely utilizes novel artificial muscles and incorporates camera for visual information processing. The actuation characteristics of the novel artificial muscles in water are presented which can be used for any other applications. The bio-inspired robot, Jelly-Z, has the following characteristics: (1) The integration of three 60 mm-long twisted, and coiled polymer fishing line (TCP$_{FL}$) muscles in a silicone bell to achieve contraction and expansion motions for swimming; (2) A Jevois camera is mounted on Jelly-Z to perform object detection while swimming using a pre-trained neural network; (3) Jelly-Z weighs a total of 215 g with all its components and is capable of swimming 360 mm in 63 seconds. The present work shows, for the first time, the integration of camera detection and TCP$_{FL}$ actuators in an underwater soft jellyfish robot, and the associated performance characteristics. This kind of robot can be a good platform for monitoring of aquatic environment either for detection of objects by estimating the percentage of similarity to pre-trained network or by mounting sensors to monitor water quality when fully developed.

1. INTRODUCTION

In recent times dealing with inhospitable environments has become inevitable. The advancement of technology and increase in demand have forced humans to consider exploration, operation, and data collection in places that are nearly impossible for them to operate in unless equipped with expensive, and in some cases, heavy protective equipment. The human activities are restrained especially in an underwater medium. They are faced with environment limitation such as extreme temperatures (4 °C to 1 °C), radiation, and extreme pressure at depths of over (10,000 ft). Moreover, facing physical limitations such as time spent underwater, size, danger when faced with underwater creatures. Adaptability is needed to deal with the numerous obstacles presented for humans in an aquatic environment, thus the integration of underwater soft robotics is highly critical and essential for the success of human exploration of the ocean.

Any soft robot's development requires improvement in its locomotion, size, weight, flexibility, and control. Combining soft materials and artificial muscles along with sensors is the steppingstone of the next generation of smart biomimetic robots making them highly compliant. This part of the development stage is critical and requires many iterations and analysis. The key challenges now are control, movement, and stiffness modulation. Control of stiffness is highly essential in soft robots [1]-[4].
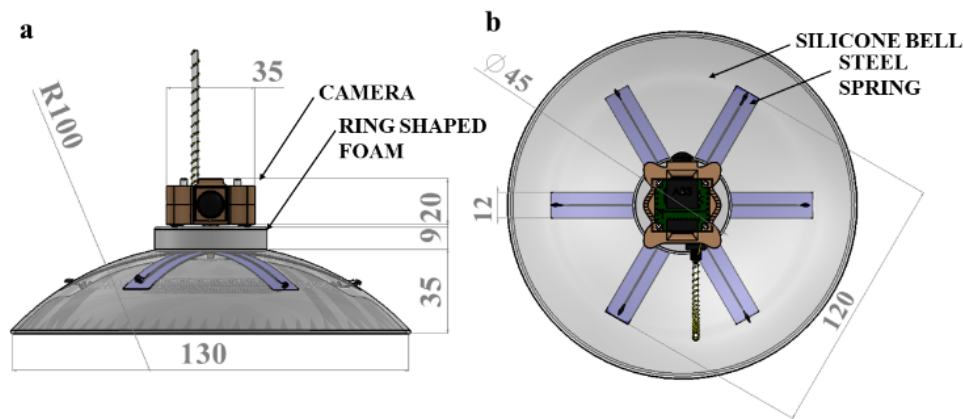
Figure 1. (a) CAD design showing major components of the Jelly-Z robot, (b) Top View.

Recently, researchers have also taken advantage of using soft material to explore the Mariana trench (depth of 11,034 m underwater) [5]. Many works have been presented which start replicating the movement and behaviour of animals using synthetic materials to illustrate a high degree of freedom robot and variability in stiffness such as 3D printed musculoskeletal joints [6], [7], biomimetic octopus like tentacles [8]-[10], robotic fish [11]-[13], and most importantly jellyfish like robots [14]-[16]. The jellyfish is considered as the most efficient swimmer in the ocean [17], with its highly flexible and deformable bell, it can propel itself long distances while exerting very low energy. Robertson et al. presented a robot with jet propulsion similar to the jellyfish inspired by scallops [18]. Origami inspired robots have also been investigated [19]. Others have presented "soft growing" robot that can be controlled and actuated with a pneumatic actuation mechanism[20]. Reviews on the challenges of maintaining linear assets by effectively utilizing autonomous robots have been shown to reduce maintenance costs, human involvement, etc. [21]. However, the research focus in our work is on the jellyfish for its geometrical simplicity and its swimming advantages. Many have also attempted to integrate artificial muscles in various configurations to achieve their desired biomimetic jellyfish design.

Some include jellyfish like robots actuated by shape memory alloys (SMAs) [14], [22], twisted and coiled polymers (TCPs) [15], dielectric elastomers (DEs) [23], [24], pneumatics [25], ionic polymer metal composites (IPMCs) [26], and hydrogen fuel powered [16]. One aspect that is missing in the literature is the integration of sensors and the lack of object detection capabilities underwater, except for a Katzschmann et al. [13] and LM-Jelly that utilizes magnetic field and electromagnetic actuator [27].

Haines et al. showed that twisted and coiled polymer muscles from fishing line (TCP_{FL}) can be very promising for robotic applications [28]. These muscles can exhibit large displacements in response to heating, which considerably decreases the stiffness of the TCP muscles [29]. The thermally induced fiber untwists in the coiled structure allowing for tensile and torsional actuation in TCP muscles [30]. Wu et al. [31] developed a novel mandrel coiled TCP_{FL} muscle for actuating the musculoskeletal system and showed that these types of actuators can be used for other soft robotic applications. However, these mandrel coiled TCP_{FL} actuators have low blocking force/ high strain; hence, taking into account to application considered in this work, we fabricated self-coiled TCP_{FL} actuators [6], [10] with large blocking force and enough displacement to actuate the soft robot.

We seek to present a fully functional swimming underwater robot, Jelly-Z, that is used for applications such as underwater monitoring and data collection. To this extent, in this work, we present Jelly-Z as shown in Figure 1, inspired by the geometry of the moon jellyfish and other similar robots, but this robot is actuated by twisted and coiled polymer fishing line muscles. It is the first jellyfish-like soft robot equipped with a camera with object detection capabilities and actuated by artificial muscles at the same time. These two features make this robot stand out as it attempts to address the fundamental problems in actuation, design, and the use of vision system of soft robots to be deployed for eco-friendly underwater mission.

The main features of this robot are:
- Mimics the bow (jellyfish bell) and string (TCP_{FL}) arrangement for the actuation mechanism.
- Noiseless and vibration free swimming underwater.
- Easy to fabricate and is lightweight.
- Equipped with a camera for surveillance and object detection underwater.

The highlights of the paper can be listed as follows. First, the detailed design and fabrication of Jelly-Z using TCP_{FL} to mimic the movement of moon jelly is shown. Second, the fabrication process and characterization results of twisted and coiled polymer fishing line muscles (TCP_{FL}) in underwater environment. Third, successful vertical swimming experiment of soft structure of Jelly-Z robot which includes swimming analysis and object detection results.

The contribution of this work in measurement and estimation is that the proposed small bioinspired underwater soft robot equipped with a small camera utilizes unique artificial muscles (which are silent in actuation, easily manufacturable and have sufficient actuation properties) for swimming. It is able to predict and detect different kinds of objects in the surrounding while swimming in water and estimating the percentage of similarity to the object the camera/robot is trained for. In addition, we provided the characteristics of the artificial muscles (TCP_{FL}) in water which can be used for other similar applications.

2. DESIGN AND FABRICATION OF JELLY-Z

The main body of Jelly-Z is fabricated from a round silicone bell (diameter 130 mm). Spring steels are added to provide stiffness to the attached artificial muscle [15, 32]. It also contains a JeVois smart camera and a piece of foam for buoyancy. A rendered image shows the assembled version of the bot in Figure 1(a and b).

2.1. Assembly of Jelly-Z robot

Unlike many rigid and complex underwater robots and ROVs Jelly-Z can be fully assembled with six simple steps. First, prepare the steel springs. The 120-micron steel spring is cut into 120 mm x 10 mm strips. Figure 2(1) shows a snapshot of one of the steel springs used in the robot. For this robot, we require a total 6 strips. Second, since the TCP$_{FL}$ muscles are directly attached to the steel strip by crimping, an insulating tape is added to prevent any current transfer between the actuating muscles and steel strip. Moreover, electrical wires are placed in between the tape and the steel strips to keep them fixed within the robot as shown in Figure 2(2). Third, a 3D printed (ABS plastic) mould (Figure 2(3)) is used to fabricate the silicone bell. The mould is prepared by cleaning its surface and spraying it with a non-stick compound. Fourth, align the steel strips in the designed direction as shown in Figure 2(4). Fifth, pour the silicone mix (EcoFlex 00-10, 1:1 ratio of part A and part B) into the mould (Figure 2(5)) and allow it to cure for a minimum of four hours. Finally, integrate the TCP$_{FL}$ muscles into the bell by attaching them to the steel springs. The artificial muscles must be stretched (pre-stressed) to create gaps between each pitch which allows it to contract while heating. Then attach both the foam and camera on the robot of the jellyfish as shown in Figure 2(6). The foam is used to set the neutral buoyancy of Jelly-Z which was calculated based on its experimental volume. The camera is also sealed and waterproofed before attaching.

2.2. Fabrication of twisted and coiled polymer fishing line (TCP$_{FL}$) muscles

The fabrication process of TCP$_{FL}$ actuators is simple, scalable, and allows the user to easily manipulate the actuator's properties such as resistance, diameter, and length. This fabrication process previously presented in detail in our previous work [6], [7], [10]. It is done in-house using a setup which includes two stepper motors, a controller, a power supply, and a computer. The fabrication consists of four major steps (1) inserting a full twist on the fishing line fibre; (2) incorporating the nichrome wire; (3) coiling the wire and nichrome together; and (4) annealing in the oven to allow the actuator to maintain its coiled structure.

To assure that all the actuators perform and behave the same, two long fishing line actuator were fabricated and later cut into the desired shorter length for the jellyfish. In this case, two 130 mm fishing line actuators were made and cut into shorter 60 mm length. The precursor fibre is an 80-lb nylon 6,6 monofilament (0.8 mm in diameter) purchased from Eagleclaw. The conductive nichrome wire is 160 μm in diameter purchased from McMaster Carr. The coiling speed was kept at 150 rpm. Figure 3 shows the fabrication set up. Stepper motor 1 (SM1) located at the top is used to insert a twist and coil the fibres.
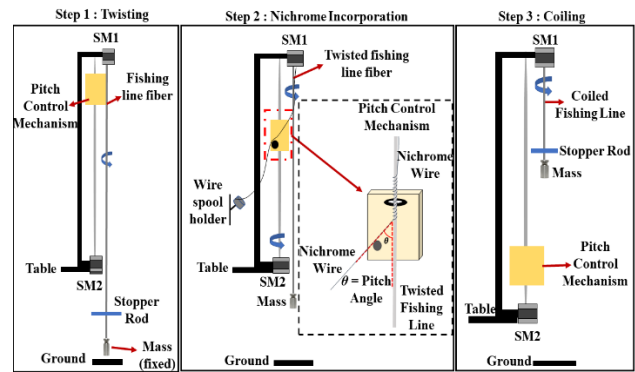
Figure 3. Schematic diagram of the TCP$_{FL}$ muscle fabrication process (left) Twisting process, (middle) Nichrome incorporation process and (right) Coiling process. Twisting and coiling protocol similar to Wu et al. [7], Hamidi et al. [6] and Almubarak et al. [10].

Stepper motor 2 (SM2) is used to guide the coiling of the nichrome wire throughout the length of the fishing line fibre. The speed of SM2 (150 rpm) is critical as it controls the pitch and amount of nichrome that is being incorporated which will affect the final electrical resistance of the actuator.

3. ISOTONIC TESTING OF TCP$_{FL}$ IN AN UNDERWATER ENVIRONMENT

3.1. Characterization Setup

Isotonic testing is one of the most important characterization processes to identify how the muscle behaves when its heated and then cooled under a constant load condition. This test can be performed in both air and underwater environment to fully mimic the muscle's true actuation condition. This set up, shown in Figure 4 (Left), includes a power supply for joule heating, NI DAQ 9219 to record the temperature change using thermocouples, and a camera along with tracker physics program to measure the displacement for an underwater testing environment.

3.2. Characterization Results

Figure 5 presents the results of the characterization experiments conducted for the TCP$_{FL}$ muscles in water. Figure 4 (right) shows a zoomed in snapshot of the TCP$_{FL}$ in its unloaded and loaded state. The length of the muscle is 60 mm (same as that in the robot), diameter D is 2.5 mm and resistance R is 60 Ω. The aim of this experiment is to test the effect of different input currents on the TCP$_{FL}$ actuator in an underwater environment. The properties of TCP$_{FL}$ muscles in water is shown in Table 1.
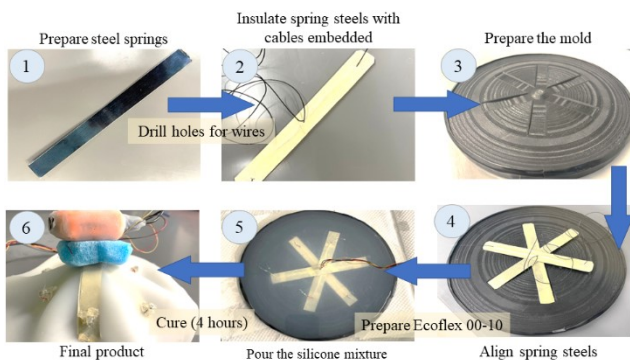
Figure 2. Schematic showing fabrication steps of Jelly-Z robot.
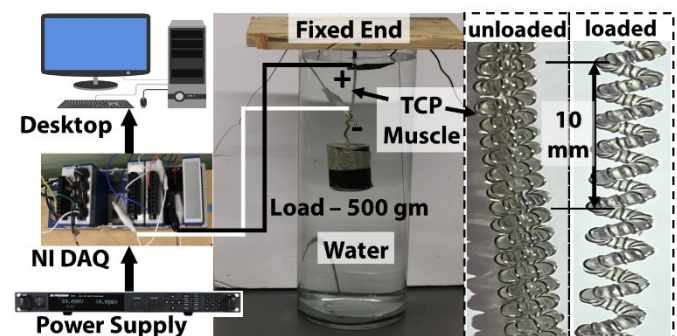
Figure 4. (Left) Isotonic test experimental setup, (Right) zoomed-in image of the TCP Fishing Line muscle; no pre-stress and with pre-stress.

Table 1. Twisted and coiled polymer fishing line actuator mechanical and electrical properties.

Property	Characteristic/Quantity
Material	Nylon (6,6) fishing line
Type of actuation	Electrothermal
Type of resistance wire	Nichrome (nickel 70 %, chromium 30 %)
Nichrome temperature coefficient of resistance (1/°C)	$579 \cdot 10^{-6}$ [33]
Fishing line diameter (mm)	0.8
Nichrome diameter (µm)	160
Length of the actuator after coiling (mm)	60
Diameter of the actuator after coiling (mm)	2
Mass of the actuator (kg)	$0.4 \cdot 10^{-3}$
Resistance (Ω)	60
Heating Time (s)	5
Cooling Time (s)	25
Duty cycle (%)	16.6
Actuation frequency (Hz)	0.33
Free strain in water (%)	~7 %
Blocking force in water (N)	5.88
Current in water (A)	0.45-0.75
Voltage (V)/ Power in water (W)	50 V / 30 W

A 500 g weight attached to the free end of the TCP$_{FL}$ muscle while the other end (top end) is fixed in a glass cylinder filled with 5.5 gallons of water. Copper wires are connected to both ends on the muscle and to a power supply. The thermocouple is directly connected to the actuator on one end and into the NI DAQ 9219 on the other. Lastly, a camera is placed at the free end on the muscle to record the displacement. A LabVIEW program collects and saves all the data at a frequency of 10 Hz for analysis by the user. The open-source tracking program (Tracker) captures the actuation displacement from the recording and the data is plotted in Matlab 2021b as shown in Figure 6.

The maximum temperature and actuation strain are measured experimentally at three different input currents (0.45 A, 0.55 A, 0.75 A) as shown in Figure 5 (a). The maximum actuation strain is noted at ~7 % (Figure 5 (d)) while the highest temperature reached is ~62 °C (Figure 5 (c)). The highest voltage consumption is ~65 V (Figure 5 (b)), which makes the power consumption ~48 W.

4. JELLY-Z SWIMMING EXPERIMENT

For efficient propulsion of the robot, pressure gradients are generated during each contraction and relaxation cycle across the bell margin of Jelly-Z bot that allows an upward movement. During each relaxation cycle there is a slight sinking of the robot due to the reverse movement of the bell. Figure 6 shows the total vertical distance Jelly-Z swam in a 70-gallon fish tank (92 x 58.5 x 46 cm³).

The jellyfish robot takes up to 21 actuation cycles to swim 360 mm vertically in 63 seconds. A camera mounted on a tripod, working at 60 fps, is used to track the Jelly-Z while swimming. The open-source tracking program (Tracker physics) is employed to measure the distance travelled by the robot and the data is plotted in Matlab 2021b. The background stripes are taken as a measurement reference as each layer (white and black in Figure 6(a)) are 8 mm wide. Three muscles of 60 mm length (60 Ω resistance each) are used to make the robot swim with an input current of 1.8 A for 1.5 s heating (contraction cycle) and
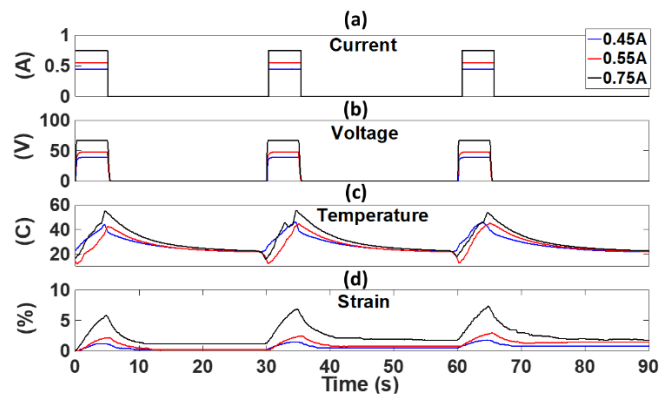
Figure 5. Experimental characterization of TCP Fishing Line muscle in an underwater environment and two-step input sequence with a pre-stress loading of 500 gm for 3 different input currents (0.45 amps, 0.55 amps, 0.75 amps); (a) Current vs Time of two-step power input, Time domain plots for two-step power input: (b) Output Voltage, (c) Temperature, (d) Strain.

1.5 s cooling (relaxation cycle – 0 A). The velocity of the robot is slower for the first 10 cycles of operation while the velocity increases as the robot reaches closer to the surface of water. This is due to the air bubbles that are formed underneath the bell as the water reacts with the high power supplied to the muscles. Figure 6(a) and Figure 6(b) show the full assembly of the Jelly-Z robot through the front and bottom perspective views.

Figure 6(c) (i, ii, iii) show the zoomed-in graphs showing the first 3 cycles (i) Current, (ii) Velocity (Velocity amplitude for each actuation cycle reaches to ~20 mm/sec.), (iii) Displacement for 0.33 Hz of actuation frequency (duty cycle – 67 %). The total electrical power used to actuate the Jelly-Z is 109.8 W, but generally these muscles consume much lesser power in air (1/3rd). This is due to the thermal energy being consumed in the surrounding environment (water); hence, to reach the actuation temperature for muscle movement, the input power is higher in water than in air. Water as a medium also allows rapid cooling of the muscles. As this is the first application shown with TCP$_{FL}$ muscles in water, more research must be conducted to reduce the heat lost in the surrounding water medium, thus reducing input power.

5. UNDERWATER OBJECT DETECTION

The experimental set up to test the design consists of a large fish tank (920 mm X 585 mm X 460 mm) made of transparent glass, a DC power supply unit, a standard laptop, a fully assembled Jelly-Z bot prototype mounted with a JeVois smart camera, and the appropriate wirings/cables for connections. For this set up, we have used JeVois A-33 Smart Camera Solution, by JeVois Smart Machine Vision (JSMV) weighing ~17 g (Figure 7, Bottom(a)). The camera (hardware specifications given in Table 2) is mounted on top of the Jelly-Z bot as shown in full assembly in Figure 7 (Top right). The camera combines with a camera sensor, embedded quad-core computer, and USB video link in a tiny package.

The advantage of using JSMV can be explained with the help of schematic in Figure 7(Bottom, (b)). A standard camera displays the output graphics without any processing and leave the analysis of data to the receiver. While a JSMV includes a processing unit which processes the video to interpret contents and provide instant results to the receiver. The hardware specifications are given in Table 2 [34].
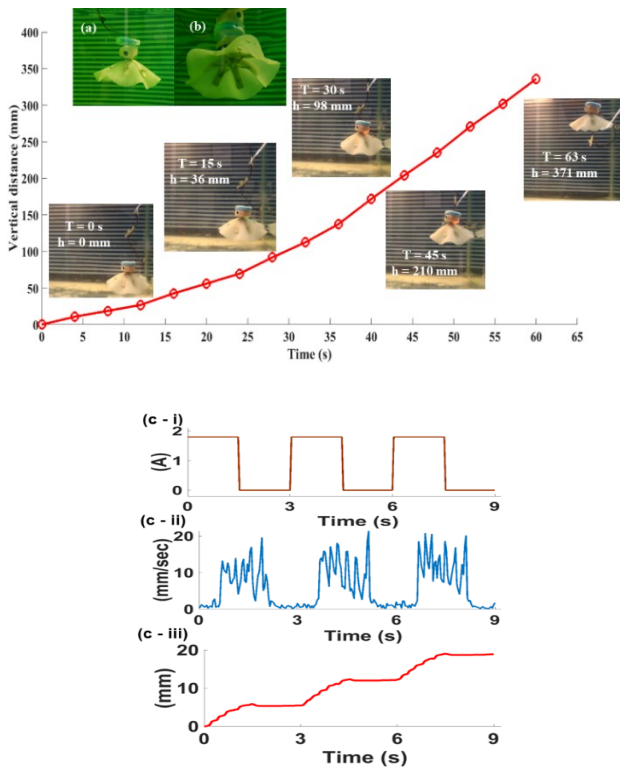
Figure 6. (*Top*) Underwater swimming analysis for Jelly-Z robot at 1.8 A input current / Voltage – 60 V, duty cycle – 50 % for an actuation frequency of 0.33 Hz at different time intervals. (a) Front perspective view. (b) Bottom perspective view. (*Bottom*) (c, i-iii) input current, velocity profile and distance vs time graphs for first three cycles.

The JSMV does not come with waterproof properties and is not suitable for underwater applications. So, in order to make the camera waterproof we have embedded the camera unit inside a silicone rubber mould, can be seen in Figure 7 (b). This allows camera to function underwater, however, the camera unit has a cooling fan which has to be removed in the process and that limits the functioning of camera up to 2 mins due to overheating.

While the software specifications include already uploaded object detection software such as TensorFlow, YOLO darknet, MatLab Module and Python Object recognition. For this set up, we have used YOLO Darknet set up. Standard Module of YOLO provided by JSMV detects upto 1000 different types of objects using deep neural network, Darknet. Darknet is an open

Table 2. Hardware Specifications of JeVois A-33 Smart Camera.

Parameters	Specifications
Weight	17 g
Size	28 cm³
Processor	Allwinner A33 quad core ARM Cortex A7 processor @ 1.34GHz with VFPv4 and NEON, and a dual core Mali-400 GPU supporting OpenGL-ES 2.0
Memory	256 MB DDR3 SDRAM
Camera sensor	1.3 MP camera with SXGA (1280 x 1024) up to 15 fps (frames/s)
Hardware serial port	5V or 3.3V (selected through VCC-IO pin) micro serial port connector to communicate with Arduino or other embedded controllers
Power	3.5 Watts maximum from USB port. Requires USB 3.0 port or Y-cable to two USB 2.0 ports.
LED	One two-color LED: Green: power is good. Orange: power is good, and camera is streaming video frames
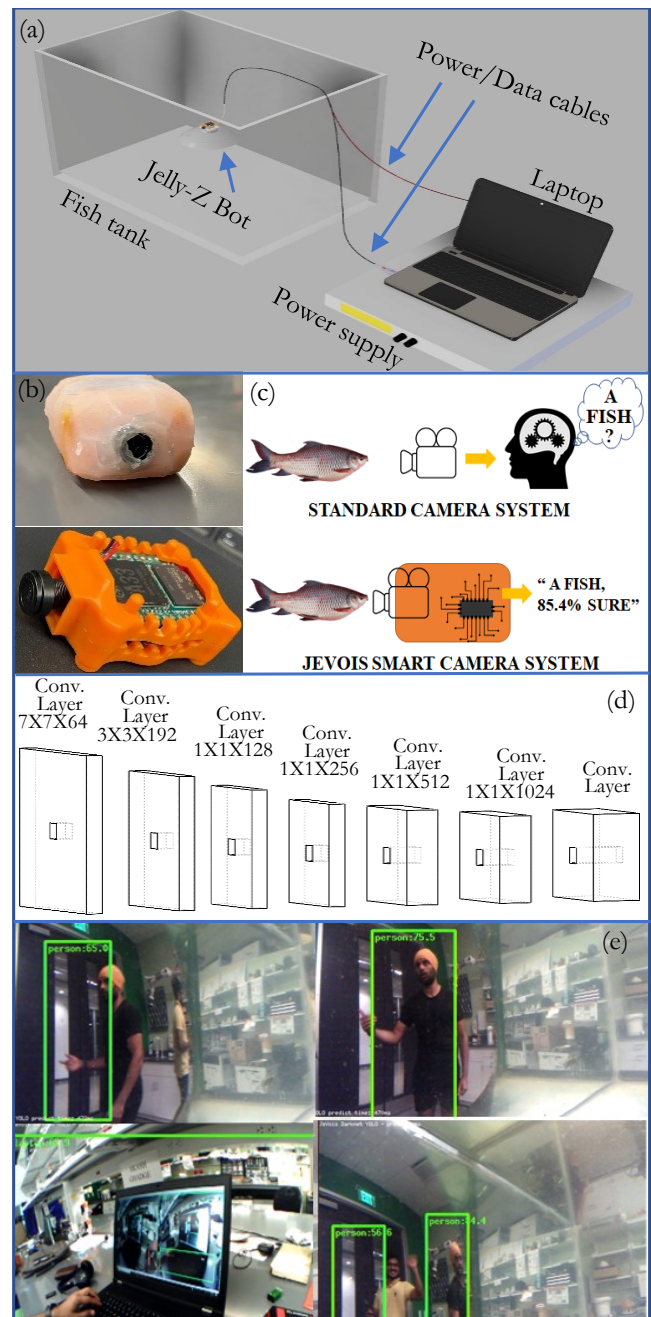
Figure 7. (a) Underwater object detection setup. (b) Waterproofing of a JeVois Camera. (c) autonomous object detection in JeVoise Camera vs Standard Camera. (d)The CNN architecture of YOLO deep learning model. (e)Experimental results of object detection from JeVois Camera. (i) 65 % Human (ii) 63% Laptop, (iii) 76% Human, (iv) Multiple Humansat 57 % & 35 %.

source neural network framework written in 'C' and 'CUDA' [35].

Figure 7(c) shows architecture of YOLO framework. YOLO's architecture is very similar to FCNN (Fully Connected Neural Network). This is a neural network that applies multiple convolutional layers to extract features from images to create learning models. The max pool layer sub-samples the image properties for each of the smaller segments in the image and trains the model accordingly. Many such layers are implemented in the neural network of YOLO. Other layers like the fully connected layer combines the weight associated to the feature properties of the image [36].

The architecture divides the sample image into a grid size of S*S, known as a residual block. Each grid cell is responsible to detect the object cantered within itself. Each grid cell predicts the bounding boxes with help of their confidence score. If there is no object in the grid cell, the confidence score would remain zero. Each bounding box provides five predictions (x, y, w, h) and confidence score. (x, y) represent the centre of the box and (w, h) represent the dimensions of the box. The predicted bounding boxes are equivalent to the true boxes of the objects when intersection over union is used. This phenomenon gets rid of any unnecessary bounding boxes that don't complement the objects' characteristics (like height and width). The final detection will be unique bounding boxes that correctly fit the objects [37].

The results of object detection experiment can be seen in Figure 7(e). The camera mounted on Jelly-Z bot while being submerged under water, can detect humans passing in-front of fish tank. The camera is also able to identify a laptop during this experiment. To test the detection of multiple objects, two people walked next to fish tank, and as seen in Figure 7(e) the camera was able to distinguish between two people and were able to detect them both separately. Capabilities of underwater detection are enormous along with application in civil and military domains.

6. CONCLUSIONS AND FUTURE WORK

We presented a fully-functional underwater jellyfish like robot, Jelly-Z. This work shows the first implementation of actuation solely by self-coiled twisted and coiled polymer with fishing line artificial muscles (TCP_{FL}) and the integration of object detection system presented for a soft underwater robot. We showed the unique design of Jelly-Z inspired by the moon jellyfish and the actuation mechanism using TCPs. This design iteration enabled the integration of three TCP_{FL} muscles for the bell contraction and relaxation motion to allow for swimming. Jelly-Z achieved swimming at a velocity of 5.7 mm/s traveling 360 mm vertically in 63 s. It could generate an instantaneous velocity of ~20 mm/s per cycle, while carrying its own weight of 215 g. It is to be noted that the vertical swimming of this robot can be controlled by turning OFF the actuation, which allows the Jelly-Z to essentially sink under the action of its own weight. Moreover, we presented the fabrication of TCP_{FL} and underwater isotonic testing. The TCP_{FL} can actuate up to ~7% in underwater condition at a power of 109 W while carrying a load of 500 g, almost 1,000 times heavier than its weight. The TCP muscles are manufactured in-house, and all the muscle integration processes are simple.

Some of the challenges to improve upon is the life cycle of these (TCP_{FL}) artificial muscles in water, the high-power consumption of the muscles and the operation time of the JeVois camera when it is underwater. These aspects need further work and should be done before considering for deployment. As for the system's behaviour in non-ideal conditions a control system will need to be developed equipped with an internal GPS and a 3D IMU which will help the robot maintain its specific position when it is pushed or exposed to high underwater currents. Autonomous underwater seakeeping is beyond the scope of the presented work but it is worth consideration for research in future projects and applications.

We also equipped Jelly-Z with the Jevois smart camera and tested for object and human detection in an underwater environment using the YOLO darknet object detection algorithm. Future work will include theoretical modelling and comparison with experimental characterization results for TCP_{FL} actuators. Improving the efficiency of TCP_{FL} actuators is another major work that has to be done in future. Water tunnel tests have to be conducted to study the generation of vortices while the robot is swimming during the contraction and relaxation motion of each cycle. Characterization of thrust force generated and simulations for the same have to be carried out from the linear robot motion for improving the efficiency of the robot design. Work has to be done on enhancing underwater imaging [37] and object detection capabilities for practical applications. The work presented here is an attempt towards developing a better design of life-like soft robotic jellyfish with no motors or rigid components for actuation.

ACKNOWLEDGEMENT

SUPPLEMENTARY

Supplementary video is available at the HBS YouTube channels; in particular, a combined video showing the structure of the robot, actuation characteristics and object detection. https://youtu.be/2MhchQribJo.

REFERENCES

[1] E. G. dos Santos, H. Richter, Design and analysis of novel actuation mechanism with controllable stiffness, Actuators 8(1) (2019), art. No. 12, pp. 1-14.
DOI: 10.3390/act8010012

[2] T. Du, J. Hughes, S. Wah, W. Matusik, D. Rus, Underwater Soft Robot Modeling and Control with Differentiable Simulation, IEEE Robotics and Automation Letters 6(3) (2021), pp. 4994-5001.
DOI: 10.1109/LRA.2021.3070305

[3] B. Lu, C. Zhou, J. Wang, Y. Fu, L. Cheng, M. Tan, Development and stiffness optimization for a flexible-tail robotic fish, IEEE Robotics and Automation Letters 7(2) (2021), pp. 834-841.
DOI: 10.1109/LRA.2021.3134748

[4] Y. Yang, Y. Li, Y. Chen, Principles and methods for stiffness modulation in soft robot design and development, Bio-Design and Manufacturing 1(1) (2018), pp. 14-25.
DOI: 10.1007/s42242-018-0001-6

[5] L. Li, X. Zheng, R. Mao, G. Xie, Energy saving of schooling robotic fish in three-dimensional formations, IEEE Robotics and Automation Letters 6(2) (2021), pp. 1694-1699.
DOI: 10.1109/LRA.2021.3059629

[6] A. Hamidi, Y. Almubarak, Y. Tadesse, Multidirectional 3D-printed functionally graded modular joint actuated by TCP_{FL} muscles for soft robots, Bio-Design and Manufacturing 2(4) (2019), pp. 256-268.
DOI: 10.1007/s42242-019-00055-6

[7] L. Wu, I. Chauhan, Y. Tadesse, A novel soft actuator for the musculoskeletal system, Advanced Materials Technologies 3(5) (2018), art. No. 1700359, pp. 1-8.
DOI: 10.1002/admt.201700359

[8] M. Calisti, M. Giorelli, G. Levy, B. Mazzolai, B. Hochner, C. Laschi, P. Dario, An octopus-bioinspired solution to movement and manipulation for soft robots, Bioinspiration & biomimetics 6(3) (2011) art. No. 036002.
DOI: 10.1088/1748-3182/6/3/036002

[9] J. Jiao, Sh. Liu, H. Deng, Yu. Lai, F. Li, T. Mei, H. Huang, Design and Fabrication of Long Soft-Robotic Elastomeric Actuator Inspired by Octopus Arm, in 2019 IEEE International

Conference on Robotics and Biomimetics (ROBIO), 06-08 December 2019, Dali, China, pp. 2826-2832.
DOI: 10.1109/ROBIO49542.2019.8961561

[10] Y. Almubarak, M. Schmutz, M. Perez, S. Shah,Y. Tadesse, Kraken: a wirelessly controlled octopus-like hybrid robot utilizing stepper motors and fishing line artificial muscle for grasping underwater, International Journal of Intelligent Robotics and Applications 6 (2022), pp. 543–563.
DOI: 10.1007/s41315-021-00219-7

[11] Z. Chen, S. Shatara, X. Tan, Modeling of biomimetic robotic fish propelled by an ionic polymer–metal composite caudal fin, IEEE/ASME Transactions on Mechatronics 15(3) (2010), pp. 448-459.
DOI: 10.1109/TMECH.2009.2027812

[12] R. Zhang, Z. Shen, Z. Wang, Ostraciiform underwater robot with segmented caudal fin, IEEE Robotics and Automation Letters 3(4) (2018), pp. 2902-2909.
DOI: 10.1109/LRA.2018.2847198

[13] R. K. Katzschmann, J. DelPreto, R. MacCurdy, D. Rus, Exploration of underwater life with an acoustically controlled soft robotic fish, Science Robotics 3(16) (2018), pp. 108-116.
DOI: 10.1126/scirobotics.aar344

[14] Y. Almubarak, M. Punnoose, N. X. Maly, A. Hamidi, Y. Tadesse, KryptoJelly: a jellyfish robot with confined, adjustable pre-stress, and easily replaceable shape memory alloy NiTi actuators, Smart Materials and Structures 29(7) (2020) art. No. 075011.
DOI: 10.1088/1361-665X/ab859d

[15] A. Hamidi, Y. Almubarak, Y. M. Rupawat, J. Warren, Y. Tadesse, Poly-Saora robotic jellyfish: swimming underwater by twisted and coiled polymer actuators, Smart Materials and Structures 29(4) (2020), art. no. 045039.
DOI: 10.1088/1361-665X/ab7738

[16] Y. Tadesse, A. Villanueva, C. Haines, D. Novitski, R. Baughman, S. Priya, Hydrogen-fuel-powered bell segments of biomimetic jellyfish, Smart Materials and Structures 21(4) (2012), art. No. 45013.
DOI: 10.1088/0964-1726/21/4/045013

[17] J. H. Costello, S. P. Colin, J. O. Dabiri, B. J. Gemmell, K. N. Lucas, K. R. Sutherland, The hydrodynamics of Jellyfish swimming, Annual Review of Marine Science 13 (2021), pp. 375-396.
DOI: 10.1146/annurev-marine-031120-091442

[18] M. A. Robertson, F. Efremov, J. Paik, RoboScallop: a bivalve inspired swimming robot, IEEE Robotics and Automation Letters 4(2) (2019), pp. 2078-2085.
DOI: 10.1109/LRA.2019.2897144

[19] Z. Yang, D. Chen, D. J. Levine, C. Sung, Origami-inspired robot that swims via jet propulsion, IEEE Robotics and Automation Letters 6(4) (2021), pp. 7145-7152.
DOI: 10.1109/LRA.2021.3097757

[20] S. Grazioso, A. Tedesco, M. Selvaggio, S. Debei, S. Chiodini, Towards the development of a cyber-physical measurement system (CPMS): case study of a bioinspired soft growing robot for remote measurement and monitoring applications, ACTA IMEKO 10(2) (2021), pp. 104-110.
DOI: 10.21014/acta_imeko.v10i2.1123

[21] D. Seneviratne, L. Ciani, M. Catelani, D. Galar, Smart maintenance and inspection of linear assets: An Industry 4.0 approach, ACTA IMEKO 7(1) (2018), pp. 50-56.
DOI: 10.21014/acta_imeko.v7i1.519

[22] A. Villanueva, C. Smith, S. Priya, A biomimetic robotic jellyfish (Robojelly) actuated by shape memory alloy composite actuators, Bioinspiration & biomimetics 6(3) (2011), art. no. 036004.
DOI: 10.1088/1748-3182/6/3/036004

[23] C. Christianson, C. Bayag, G. Li, S. Jadhav, A. Giri, Ch. Agba, T. Li, M. T. Tolley, Jellyfish-inspired Soft Robot driven by fluid

electrode dielectric organic robotic actuators, Frontiers in Robotics and AI 6 (2019), art. No. 126, pp. 1-11.
DOI: 10.3389/frobt.2019.00126

[24] T. Cheng, G. Li, Y. Liang, M. Zhang, B. Liu, T.-W. Wong, J. Forman, M. Chen, G. Wang, Y. Tao, T. Li, Untethered soft robotic jellyfish, Smart Materials and Structures 28(1) (2018), art. No. 015019, 2018.
DOI: 10.1088/1361-665X/aaed4f

[25] J. Frame, N. Lopez, O. Curet, E. D. Engeberg, Thrust force characterization of free-swimming soft robotic jellyfish, Bioinspiration & biomimetics 13(6) (2018), pp. 64001-64001.
DOI: 10.1088/1748-3190/aadcb3

[26] S.-W. Yeom, I.-K. Oh, A biomimetic jellyfish robot based on ionic polymer metal composite actuators, Smart materials and structures 18(8) (2009) art. No 085002.
DOI: 10.1088/0964-1726/18/8/085002

[27] J. Ye, Y.-Ch. Yao, J.-Y. Gao, S. Chen, P. Zhang, L. Sheng, J. Liu, LM-Jelly: Liquid metal enabled biomimetic robotic jellyfish, Soft Robotics, 2022 (in press).
DOI: 10.1089/soro.2021.0055

[28] C. S. Haines, M. D. Lima, N. Li, G. M. Spinks, J. Foroughi, J. D. W. Madden, S. H. Kim, Sh. Fang, M. Jung de Andrade, F. Göktepe, Ö. Göktepe, S. M. Mirvakili, S. Naficy, X. Lepró, J. Oh, M. E. Kozlov, S. J.Kim, X. Xu, B. J. Swedlove, G. G. Wallace, R. H. Baughman, Artificial muscles from fishing line and dewing thread, Science 343(6173) (2014), pp. 868-872.
DOI: 10.1126/science.1246906

[29] Y. Tadesse, L. Wu, F. Karami, A. Hamidi, Biorobotic systems design and development using TCP muscles, Proc. SPIE 10594, Electroactive Polymer Actuators and Devices (EAPAD) XX, 1059417 (2018).
DOI: 10.1117/12.2300943

[30] J. A. Lee, N. Li, C. S. Haines, K. J. Kim, X. Lepró, R. Ovalle-Robles, S. J. Kim, R. H. Baughman, Electrochemically Powered, Energy-Conserving Carbon Nanotube Artificial Muscles Advanced materials (Deerfield Beach, Fla.) 29(31) (2017), art. No. 1700870.
DOI: 10.1002/adma.201700870

[31] L. Wu, I. Chauhan, Y. Tadesse, A novel doft actuator for the Musculoskeletal system, Adcanced Material Technologies 3(5) (2018), art. No. 1700359, pp. 1-8.
DOI: 10.1002/admt.201700359

[32] Y. Almubarak, M. Punnoose, N. X. Maly, A. Hamidi, Y. Tadesse, KryptoJelly: a jellyfish robot with confined, adjustable pre-stress, and easily replaceable shape memory alloy NiTi actuators (2020), art. No. 075011.
DOI: 10.1088/1361-665X/ab859d

[33] MatWeb. Nichrome 70-30 Medium Temperature Resistor Material. Online [Accessed 23 August 2022]
http://www.matweb.com

[34] i. a. t. U. o. S. C. Laurent Itti. (2016). JeVois Smart Machine Vision Camera. Online [Accessed 23 August 2022]
http://jevois.org/

[35] J. Du, Understanding of object detection based on CNN family and YOLO, Journal of Physics: Conference Series 1004 (2018), art. No. 012029.
DOI: 10.1088/1742-6596/1004/1/012029

[36] M. Asyraf, I. Isa, M. Marzuki, S. Sulaiman, C. Hung, CNN-based YOLOv3 comparison for underwater object detection, Journal of Electrical & Electronic Systems Research 18 (2021), pp. 30-37.
DOI: 10.24191/jeesr.v18i1.005

[37] W. Gai, Y. Liu, J. Zhang, G. Jing, An improved Tiny YOLOv3 for real-time object detection, Systems Science & Control Engineering 9(1) (2021), pp. 314-321.
DOI: 10.1080/21642583.2021.1901156